

**ANTIMICROBIAL ACTIVITY OF NOVEL POROUS  $ZnGd_2O_4$   
NANOPARTICLES EXHIBIT NANOPARTICLE-BACTERIA INTERFACE**

**M. C. Naik**

Department of Chemistry,  
Smt.K.W.College, Sangli,  
(M.S.)-416416, India

**S. R. Bamane**

Raja Shripatrao Bhagwantrao College,  
Aundh, Satara, India

**Abstract :**

*The porous and novel  $ZnGd_2O_4$  nanoparticles with oval morphology were synthesized by simple combustion method. The presence of wurtzite  $ZnO$  nanophase with  $Gd_2O_3$  spinel nanoparticles inside  $ZnGd_2O_4$  were confirmed by the use of XRD pattern and supportive FTIR spectrum. XRD data proved phase purity of the nanomaterial. These porous nanoparticles had shown good surface activity and stability on the basis of thermal analysis. The elemental composition and porous nature of these nanoparticles were confirmed on the basis of SEM-EDAX analysis. The 55 nm. size of these nanoparticles was matched with TEM-SAED pattern. These porous metal oxide nanoparticles had exhibited good surface activity and biocompatibility on the basis of antimicrobial screening on gram positive and gram negative bacteria. Hence these nanoparticles find applications in future biomedical and sensing fields.*

**Keywords :** Porous  $ZnGd_2O_4$  nanoparticles, antimicrobial, surface activity.

**1. Introduction :**

Porous nanoparticles generally show good surface activity and can bind with various chemical functional groups. Zinc oxide nanoparticles are showing variety of applications in electronics, biomedical and engineering field due to their versatile physical and electronic properties with good stability. The gadolinite nanoparticles

similar to ferrite materials are recently focused for use in sensing and biological fields due to their extra stability and good luminescent and porous nature. The gadolinite  $\text{ZnGd}_2\text{O}_4$  is exhibiting the presence of  $\text{ZnO}$  and  $\text{Gd}_2\text{O}_3$  phases.  $\text{Gd}_2\text{O}_3$  nanoparticles had shown good biological and electronic properties. Recent trend in novel metal oxide nanoparticles throws light on synthesis of porous gadolinium and zinc based mix metal oxide nanoparticles for variety of sensing and biomedical applications.

Aruguete D.M. et. al have explained use of nanoparticles in antimicrobial applications and also thrown light on their effects in nanotoxicology [3]. Raghupati K.R., Koodali R.T. and others have discussed the effects of sizes of nanoparticles on antibacterial activity especially with reference of  $\text{ZnO}$  nanoparticles [7]. Tran N. et. al. have realized the effects of magnetism and surface activity of iron based nanoparticles on antibacterial action of gram positive bacteria [9]. Arekha M. et. al have estimated the fact of bacteria and nanoparticle surface action with the use of iron oxide based nanoparticles for better antibacterial effects [11]. All these report suggest that the surface, size and nature of nanoparticles affect on antimicrobial activities, which are mainly based on cell-particle interactions of nanoparticle surfaces with bacteria.  $\text{ZnO}$  and gadolinium based nanoparticles are now used for biomedical applications because these nanoparticles are porous and magnetoluminescent to attract cell surface and chemically binds with cell membranes due to their robust magnetism and porosity. Babayevska N., Wozniak A. et. al. had synthesized  $\text{ZnO@Gd}_2\text{O}_3$  nanoparticles for biomedical applications on the basis of their surface reactivity and luminescence [1], whereas Babayevska N., Florczak P. et. al. had studied their applications as contrast agent in biomedical fields [2]. Hence zinc doped gadolinium oxide nanoparticles had got attention in nano biotechnology. Here on the basis of the recent surge of synthesis of novel mixed metal oxide nanoparticles, we had synthesized novel  $\text{ZnGd}_2\text{O}_4$  nanoparticles

by simple combustion method and confirmed their surface reactivity for cell effusion and future sensing potential on the basis of antimicrobial screening.

## 2. Experimental section:

**Materials :** All the chemicals used for synthesis of gadolinite,  $\text{ZnGd}_2\text{O}_4$  nanoparticles and their biological screening such as gadolinium nitrate hexahydrate, zinc nitrate, urea as fuel were of A. R. grade, which were purchased from S. D. fine chem. Ltd. and Merck ltd and were used without further purification. The cell culture medium as agar and bacterial culture were obtained from Himedia. The double distilled water was obtained from Millipore system and used throughout the synthesis and biological screening tests.

### **Synthesis of novel porous $\text{ZnGd}_2\text{O}_4$ nanoparticles by combustion method :**

The novel and porous  $\text{ZnGd}_2\text{O}_4$  gadolinite nanoparticles were synthesized by using simple and handy combustion method. Briefly, 0.01 M zinc nitrate hexahydrate and 0.02 M gadolinium nitrate salts were mixed together in a Borocil beaker and kept for constant heating over hotplate in ambient air atmosphere. Then 2 folds of about 0.04 M urea is added as fuel for complete combustion of salt mixture to yield bare metal oxide nanoparticles. Then the nanoparticles were ignited in alumina crucible in a muffle furnace for 3 hours at  $650^\circ\text{C}$  at ignition temperature determined on the basis of TG-DTA thermal analysis. The porous metal oxide nanoparticles obtained with better powder nature and good stability were used for further physicochemical and biological analysis.

### **Structural and morphological characterization of $\text{ZnGd}_2\text{O}_4$ nanoparticles :**

The structure, morphology, particle sizes and types of atoms in the composition of gadolinite  $\text{ZnGd}_2\text{O}_4$  nanoparticles were confirmed by physicochemical characterization on the basis of FTIR, XRD spectral analysis, TEM and SEM-EDAX microscopic and elemental analysis. The stability and surface activity of these nanoparticles were estimated by TG-DTA thermal analysis. FTIR spectra of nanoparticles was determined using KBr pallet method on Perkin Elmer series

spectrometer. While XRD pattern of bare ignited nanoparticles was determined using powder XRD technique with Cu K $\alpha$  line source. Jeul SEM-EDAX and Jasco TEM microscopic instruments are utilized for determination of morphologies and electron diffraction patterns of gadolinite nanoparticles to confirm data with XRD observations.

### **Antimicrobial screening of porous ZnGd<sub>2</sub>O<sub>4</sub> nanoparticles :**

The cell-particle interactions of nanomaterials elaborating their surface reactivity and biocompatibility can be studied only using simple *in vitro* antibacterial screening in buffer solutions to maintain physiological mimicking pH at nanoparticle cell interactions. Here we have tested the antimicrobial activity and surface biocompatibility of new ZnGd<sub>2</sub>O<sub>4</sub> nanoparticles on gram positive and gram negative bacteria by Agar well method. Briefly, .....ppm. doses of nanoparticles in phosphate buffer (physiological pH=7.4) are exposed to bacterial agar cell culture in wells bored with 2 to 4 mm. diameters on culture plates. Then the cultures are incubated for 8 and 12 hours in dark. After incubation plates are opened from cover and zones of inhibition of microbial culture are related to biocompatibility of nanoparticles to study further mechanism of endocytosis inside bacterial cells with cell-nanoparticle interactions of these novel porous gadolinite family nanoparticles.

### **3. Results and Discussion:**

#### **Morphological and structural characterization of ZnGd<sub>2</sub>O<sub>4</sub> nanoparticles :**

##### **FTIR spectrum :**

The FTIR spectra of ZnGd<sub>2</sub>O<sub>4</sub> nanoparticles had shown peaks in both the regions of functional and fingerprint signals. The fingerprint group signal region of the FTIR spectra had exhibited the presence of ZnO and Gd<sub>2</sub>O<sub>3</sub> phase system, while functional region of spectral signals had shown presence of spinal and wurtzite phases with Zn-O-Zn, Gd-O-Gd and Zn-Gd vibrations. The FTIR spectra of these nanoparticles have shown peak frequency at 3570 cm<sup>-1</sup> which evidenced for the presence of surface -OH groups of porous gadolinite nanoparticles. Peaks at 1450

$\text{cm}^{-1}$  and  $1750 \text{ cm}^{-1}$  had shown presence of Zn-O-Zn and Gd-O-Gd bonded groups of  $\text{Zn}^{2+}$  and  $\text{Gd}^{3+}$  ions with oxide ions in nanoparticle lattice. The peak at  $450 \text{ cm}^{-1}$  may be attributed to Zn-Gd vibrations. All other peaks of FTIR spectra of nanoparticles confirm presence of cubic and hexagonal phases in lattice of gadolinite nanoparticles (refer fig. 1A). Hence it was evidenced from these FTIR signals that, the nanoparticles contain phase purity porous nature and atmospheric moisture on their surfaces.

**TG-DTA thermal analysis :** TG-DTA analysis had performed to elaborate the surface weight loss relating to stability, porosity and reactivity with water and wetability entrapment efficiencies TGA plots as per formula:

**Surface moisture entrapment** = % weight loss for drug / % weight loss of nanocomposites X 10

As per table 1, after thermal analysis and *in vitro* MTT cell line assay for nanocomposites, it was proved that thermal analysis support the biological interactions of nanocomposites as surface interaction of nanomaterials with cells. DTA analysis of nanocomposites in figures 2 and 4 proves the more chemical changes than physical transitions for surfaces of nanoparticles due to release of enthalpies in negative side peaks in DTA curves. So this observation supports activity of surfaces of nanocomposites on the basis of TG-DTA analysis.

Table 1 : Comparison of drug delivery ability of nanocomposites.

TG-DTA stability temperature From weight loss	Weight loss at TGA curve	Physical changes at surface	Chemical changes at surface
bare $\text{ZnGd}_2\text{O}_4$ ( $^{\circ}\text{C}$ )	26 %	Surface phase change to crystalline	Loss of surface $\text{H}_2\text{O}$

		porosity	and CO <sub>2</sub>
--	--	----------	---------------------

Higher drug entrapment, drug delivery were observed for PEG-cyclodextrin coating on ferrite nanoparticles than chitosan coating supported by TG-DTA thermal analysis. Hence thermal properties of nanocomposites are related to surface profiling and drug loading and delivery potentials (fig. 7A and 7B).

### XRD (X ray diffraction) pattern of nanoparticles:

As per fig. 2 representing XRD spectra of synthesized amorphous, porous and pure ZnGd<sub>2</sub>O<sub>4</sub> nanoparticles, a high intense strong and broad peak is obtained in XRD spectra, which have proved the presence of single phase purity of nanoparticles as spinal Gd<sub>2</sub>O<sub>3</sub> with wurtzite ZnO phase. The crystallite sizes of the gadolinite nanoparticles are then determined by Scherrer's formula as,  $K = 0.9\lambda/\beta \cdot \cos\theta = 50-58$  nm. (54 nm. from main diffraction peak) Where,  $\beta$ = FWHM of peaks,  $\lambda$ = 1.54 nm.,  $\theta$ = diffraction angle, and K= crystallite size. But as XRD peaks are slightly blurred and broad representing the amorphous and porous nature. The miller indices, lattice planes and constants representing gadolinite nanocrystals are confirmed with data of JCPDS card no. as per table1 as follows,

Table 1 : Crystal parameters of gadolinite nanoparticles matched with standard JCPDS card.

Crystallite planes (Miller Indices) (h,k,l) Hexagonal wurtzite and spinal phase	d Calculated A <sup>0</sup> $d = a/\sqrt{(h^2 + k^2 + l^2)}$ or $2d\sin\theta = n\lambda$	d Standard A <sup>0</sup> JCPDS card no.- 36-1451	Lattice Constant a A <sup>0</sup> from main XRD peak of bare ZnGd <sub>2</sub> O <sub>4</sub>
100	3.2510	3.2490	a standard = 3.249
002	1.6255	1.6245	
<b>101</b>	2.2988	2.2974	
102	1.4539	1.4530	a calculated =

110	2.2988	2.2974	3.251
103	1.0280	1.0274	

### TEM image and SAED pattern of nanoparticles :

The TEM images of gadolinite nanoparticles were exhibited oval morphology and sizes between 45 to 60 nm. which were matched with mean crystallite size of XRD spectra as 54 nm.. Hence the sizes of these nanoparticles were ranged from 50 to 54 nm. (refer fig. 4 TEM image and SAED pattern). SAED pattern of nanoparticles had shown dots representing electron diffraction of planes in crystals. As these patterns of dots are some diffused it proves the slight amorphous surface porous nature of nanoparticles. The TEM image of nanoparticles represent oval shapes and some porous surface to surface agglomerations elaborating their slight amorphous phases.

### SEM and EDAX patterns :

SEM image of  $\text{ZnGd}_2\text{O}_4$  nanoparticles shows porous nature of nanomaterial (refer fig. 3A ). The nanoparticles exhibit oval shapes and high porosity for their surface activity. Along with SEM imaging of the nanoparticles EDAX analysis had been performed to confirm the elemental composition. The EDAX pattern shows presence Gd, Zn and abundant oxygen atoms. As per XRD observations  $\text{Gd}^{3+}$  ions occupy tetrahedral and octahedral positions in nanoparticle porous crystals, while  $\text{Zn}^{2+}$  ions occupy tetrahedral positions in lattice. This observation was supported by EDAX patterns on the basis of electron diffraction energies and intensities of peaks (Fig. 3B). Hence hexagonal and spinal phases of gadolinite nanocrystal had been confirmed here.

### Antimicrobial properties of gadolinite nanoparticles elaborating surface porosity :

Table 2: antimicrobial activities of gadolinite  $\text{ZnGd}_2\text{O}_4$  nanoparticles on gram positive and gram negative bacteria compared by agar well assay and exhibited comparatively in fig. 5A to 5H.

Concentrations of drug/ dose of ZnGd <sub>2</sub> O <sub>4</sub> in phosphate buffer µg./ml. (ppm.) <i>in vitro</i> on bacterial cells	Zones of inhibition for gram positive bacteria in zone diameter mm. on <i>Staph. Aureus</i>		Zones of inhibition for gram negative bacteria in zone diameter mm. on <i>E</i> <i>Coli.</i>	
	After 8 hours incubation	After 12 hours incubation	After 8 hours incubation	After 12 hours incubation
5	62	38	14	86
10	78	22	18	82

### Mechanism for surface reactivity of nanoparticles on the basis of cell particle interactions:

As per scheme 1, when gadolinite nanoparticles with good porosity enters into bacterial cell membranes, the ZnGd<sub>2</sub>O<sub>4</sub> nanoparticles attract functional groups of negatively charged cell membranes such as -NH<sub>2</sub>, -COO, -OH due to magnetic nature of Gd<sup>3+</sup> ions in the nanoparticles containing 7 unpaired electrons. As these nanoparticles have oval shapes and surface porosity, the nanoparticles at physiological pH are prone to endocytosis in bacterial cells by chemical interactions and surface bonding. Hence these nanoparticles show surface reactivity and probable watability with bacterial cell membranes. Overall these nanoparticles are biocompatible to gram positive and gram negative bacteria with more antimicrobial action on gram negative bacteria with some luminescence emission. When these novel porous gadolinite nanoparticles get endocytized in bacterial cell membranes, lysosomal enzymes degrade porous surfaces of the nanoparticles releasing Zn<sup>2+</sup> and Gd<sup>3+</sup> ions with production of ROS (reactive oxygen species) like O<sup>•</sup>, OH<sup>•</sup>, OOH<sup>•</sup> and H<sub>2</sub>O<sub>2</sub>. The ROS produced inside bacterial cells by these porous nanoparticles on the basis of cell nanoparticle interaction enter into rough organelles and mitochondria of cells disturbing membrane potentials of cell



organelles and damage DNA and RNAs as per reference [12]. Finely these nanoparticles cause lipid peroxidation (LPO) of bacterial cells giving cell damage and cell growth inhibitions. Thus the porous gadolinite nanoparticles fastly cause antimicrobial action due to surface porosity mostly against gram negative bacteria.

#### 4. Conclusions :

The novel and porous  $\text{ZnGd}_2\text{O}_4$  nanoparticles were synthesized by simple combustion route and exhibited oval shapes. These nanoparticles had shown good surface reactivity and stability on the basis of thermal analysis and antimicrobial screening. The phase purity and crystal packing of these nanoparticles were confirmed by XRD analysis. The oval morphology, surface porosity, composition and spinal and hexagonal nanophases inside the nanoparticles were confirmed with TEM-SAED and SEM-EDAX patterns and data was matched with XRD elaborations. These nanoparticles had shown presence of wurtzite ZnO and Spinal cubic  $\text{Gd}_2\text{O}_3$  nanophase structures. These gadolinite nanoparticles had exhibited good antibacterial activity on gram positive and gram negative bacteria elaborating their porous surface physicochemical interactions with negative charged cell membranes. On the basis of these observations the nanoparticles had shown cell particle adsorption effects on surfaces. So these novel and porous gadolinite nanoparticles finds better applications in sensing and biomedical fields.

**5. Acknowledgements:** The authors are thankful to NCL laboratory Pune, India for providing some electron microscopic characterizations.

#### 6. References :

- [1] Babayevska N., Wozniak A., Grzeskowiak B.F., Wiveger M., Stomski R., Zalewski T., Drobna M., Woznaik Bunych M., Jurga S., “ZnO@Gd<sub>2</sub>O<sub>3</sub> core/ shell nanoparticles for biomedical applications : physicichemical, in vitro and in vivo characterization”, *Mat. Sci. Engi.-C*, **2017**, 80, 603-615.
- [2] Babayevska N., Florczak P., Woznaik-Bunych M., Jarek M., Mwachyk G., Zalewski T., Jurga S., “Functionalized multimodal ZnO@Gd<sub>2</sub>O<sub>3</sub>

- nanosystems to use as perspective contrast agent for MRI”, *Appl. Surf. Sci.*, **2017**, 404, 129-137.
- [3] Aruguete D.M. et. al., “Antimicrobial nanotechnology: its potential for the effective management of microbial drug resistance and implications for research needs in microbial nanotoxicology”, *Env. Sci. : process and impacts*, **2013**, 15, 93-102.
- [4] Zhu X., Radovik-Moreno A.F., Wu J., Langer R., Shi J., “Nanomedicine in the management of microbial infection –overview and perspectives”, *Nano today*, **2014**, 9, 478-498.
- [5] Zhang L., Pornpattananankul D., Hu C.M., Huang C.M., “Development of nanoparticles for anti microbial drug delivery”, *Curr. Med. Chem.*, **2010**, 17, 585-594.
- [6] Seil J.T., Webster T.J., “Antimicrobial applications of nanotechnology : methods and literature”, *Int. J. Nanomed.*, **2012**, 7, 2767.
- [7] Raghupati K.R., Koodali R.T., Manna A.C., “Size dependant bacterial growth inhibition and mechanism of antibacterial activity of zinc oxide nanoparticles”, *Langmuir*, **2011**, 27, 4020-4028.
- [8] Hajipour M.J. et. al., “Antibacterial properties of nanoparticles”, *trends in biotech.*, **2012**, 30, 499-511.
- [9] Tran N. et. al., “Bactericidal effect of iron oxide nanoparticles on *Staphylococcus aureus*”, *Int. J. Nanomed.*, **2010**, 5, 277.
- [10] Jin T., He. Y., “Antibacterial activities of magnesium oxide (MgO) nanoparticles against foodborne pathogens”, *J. Nanopart. Res.*, **2011**, 13, 6877-6885.
- [11] Arekha M. et. al., “Antimicrobial activity of iron oxide nanoparticle upon modulation of nanoparticle -bacteria interface”, *Sci. rep.*, **2015**, 5.
- [12] Alpaslan E., Geilich B.M., Yazici H., Webster T.J., “pH-controlled cerium oxide nanoparticle inhibition of both gram-positive and gram-negative bacterial growth”, *Sci. rep.*, **2017**, 7.

**Figure captions:**

**Figure 1A :** FTIR spectrum of bare  $\text{ZnGd}_2\text{O}_4$  nanoparticles

**Figure 1B :** TGA and DTA plot of bare  $\text{ZnGd}_2\text{O}_4$  nanoparticles

**Figure 2 :** XRD pattern of porous nanometal oxide  $\text{ZnGd}_2\text{O}_4$  with wurtzite and spinal packing (Z3).

**Figure 3A :** SEM and **3B:** EDAX pattern of bare  $\text{ZnGd}_2\text{O}_4$

**Figure 4 :** TEM image and SAED patterns of  $\text{ZnGd}_2\text{O}_4$  matched with XRD data.

**Figure 5A to 5H :** Antibacterial activity of porous  $\text{ZnGd}_2\text{O}_4$  on gram positive (*Staph. Aureus*, *Pseudomonas*) bacteria and gramnegative bacteria (*E. Coli*)

**Scheme 1 :** Mechanism for antimicrobial effects of porous gadolinite nanoparticles on the basis of nanoparticle surface-cell interactions.

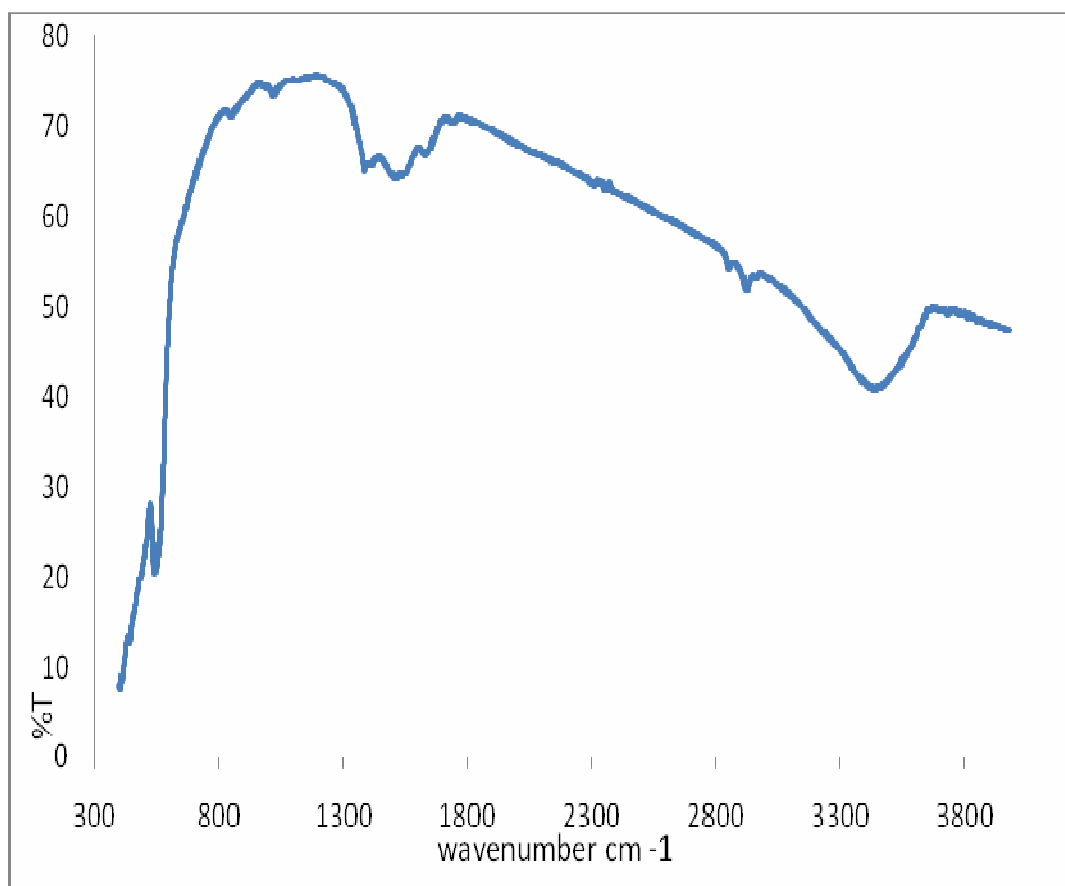


**Figure 1A**

Figure 1B

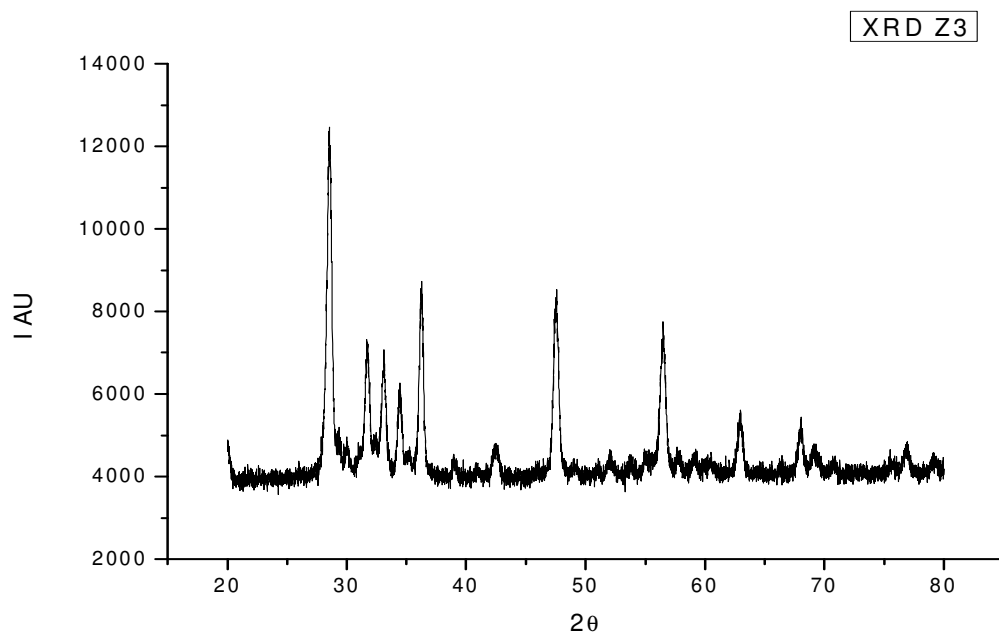


Figure 2

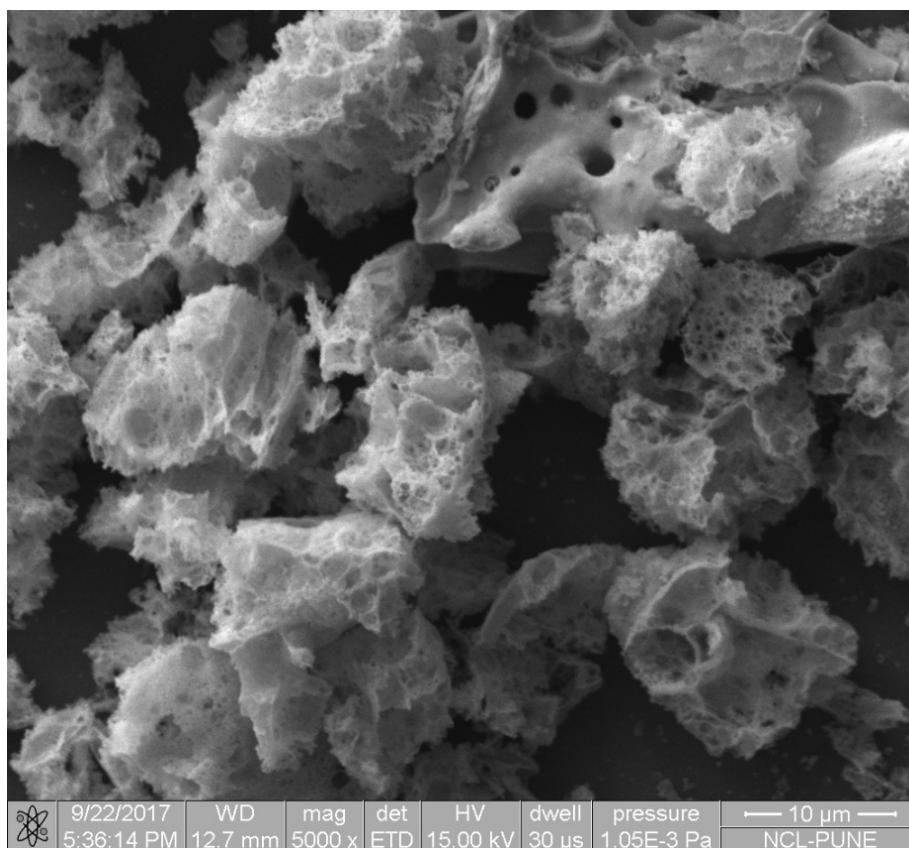


Figure 3A

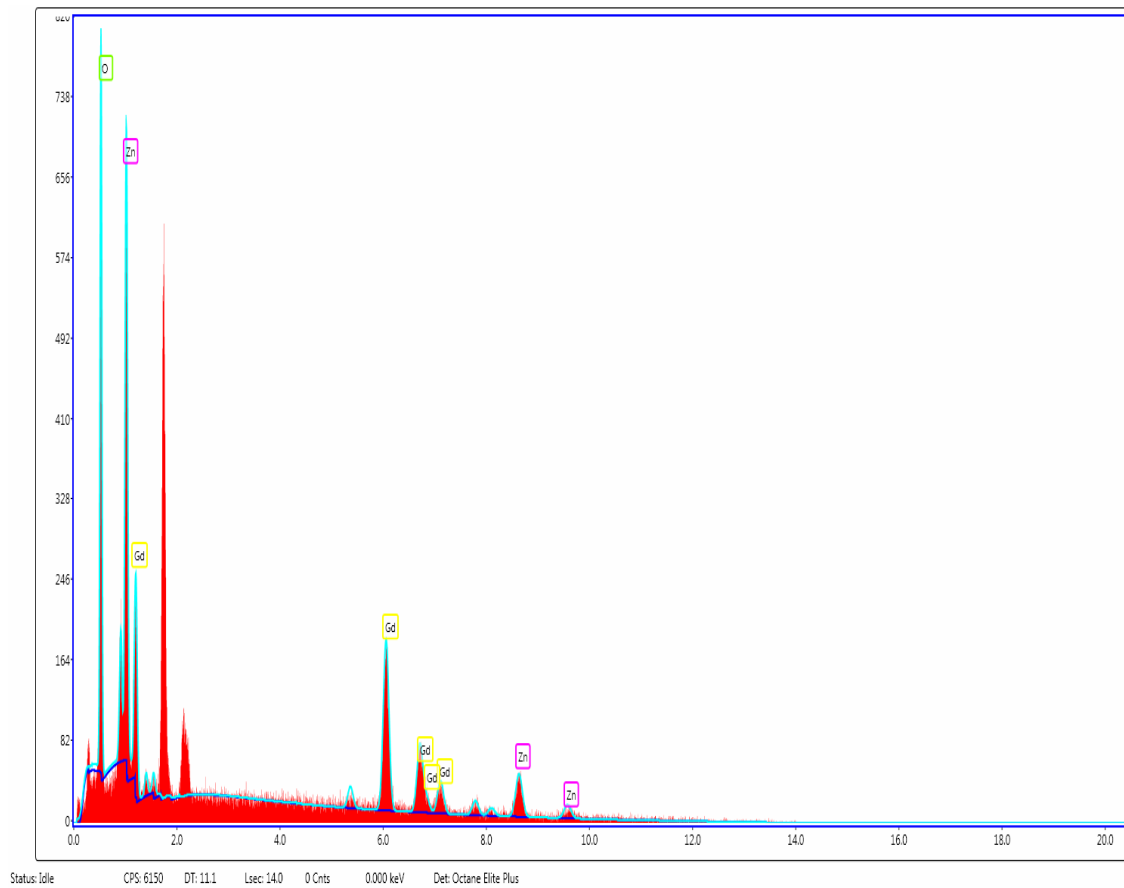


Figure 3B

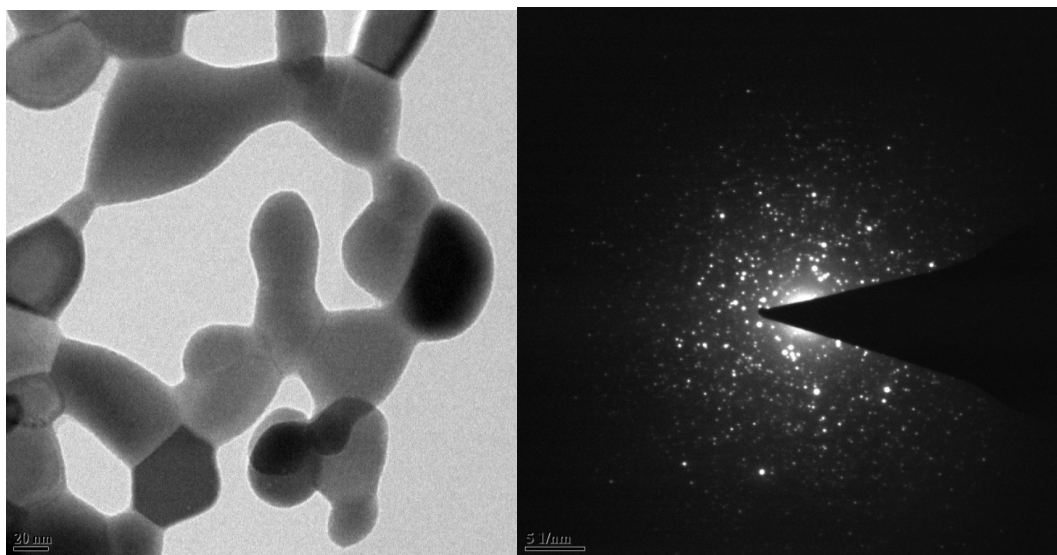


Figure 4

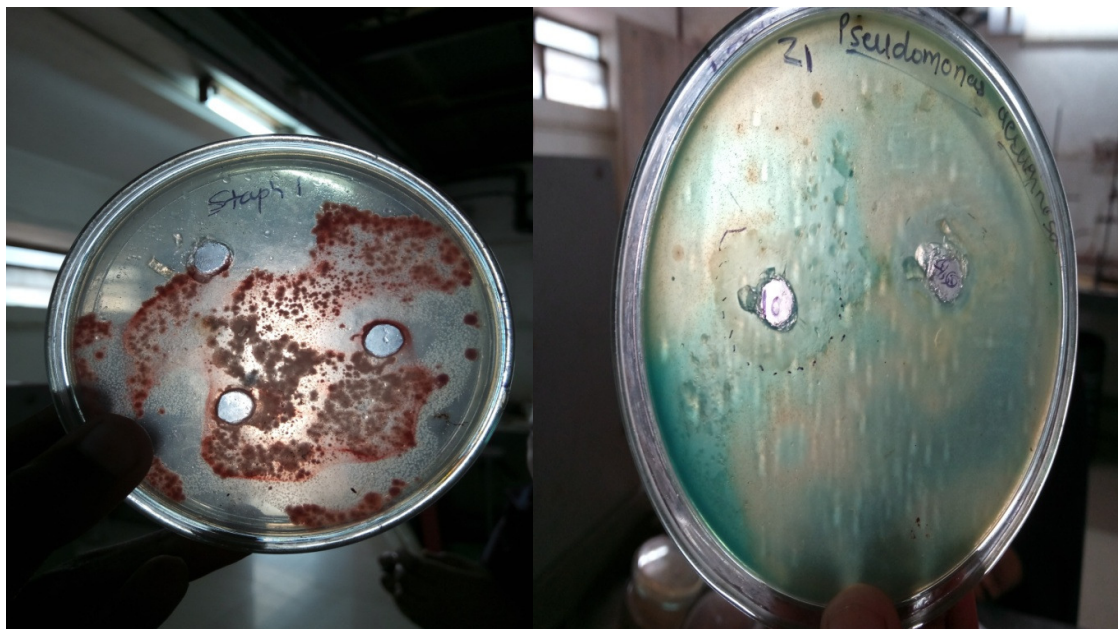
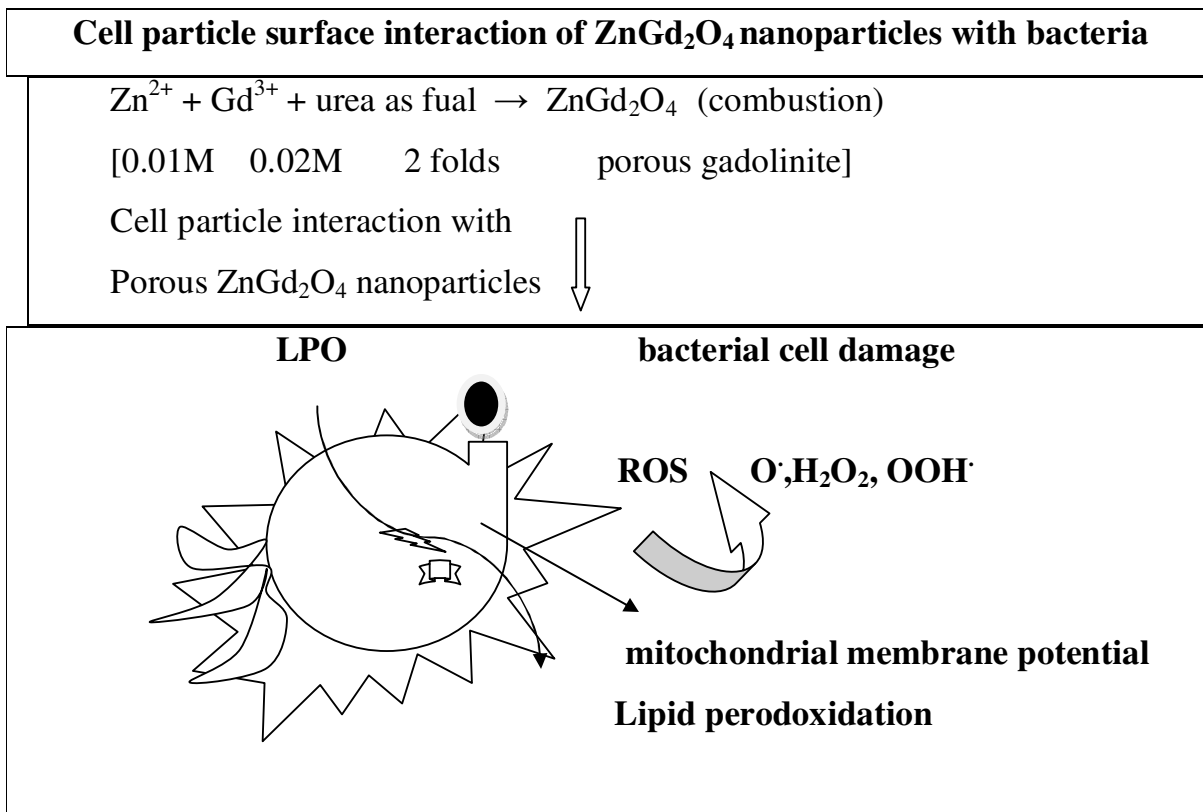


Figure 5A to 5D

Figure 5E to 5H



Scheme 1

Graphical abstract:

